viously.[2] Two check reflections remained stable throughout data collection. Because of uncertainty in background levels, which affected weak reflections most seriously, only data with $I > 4\sigma(I)$ were included in later calculations.

The positions of the two rhodium atoms and one tin atom were determined by direct methods. The remaining atoms, except for hydrogen, were located on successive difference maps. Two solvent molecules were found, one well behaved and the other with signs of severe disorder. The disordered molecule was included as nine chlorine atom fragments, with occupancy factors from 0.15 to 0.4. No peak here could be reasonably attributed to carbon.

Following convergence of refinement with isotropic temperature factors, an empirical absorption correction was applied.[28] Final refinements were carried out with anisitropic temperature factors for all atoms heavier than nitrogen, with the exception of the disordered chlorine atoms. Hydrogen atoms were included in calculated positions. The chirality of the crystal was determined by comparing R and goodness of fit for the two "hands"; the reference parameters were obtained from a refinement with all f'' set to 0.

Final block-cascade refinement of 450 parameters converged with $R = 0.049$, average positional esd's for Rh, Sn 0.002; P, Cl 0.004; C, N, O 0.01–0.015 Å. A final difference map showed a peak of 1.4 eÅ^{-1} near Rh(2) and some smaller peaks (~0.5 eÅ^{-1}) in the region of the disordered solvent molecule.

All calculations were carried out on a Data General Eclipse computer, with local programs for data reduction and absorption correction[28] and SHELXTL for solution, refinement, molecular geometry, and graphics. The form factors, including anomalous scattering, were from the International Tables.[29]

Acknowledgment. We thank the National Science Foundation (CHE 8217954) for support. F.E.W. was a University of California Regents Fellow.

Registry No. 3, 98652-01-8; **4**, 98717-42-1; **5**, 98652-02-9; **6**, PF_6, 87555-69-9; $Rh_2(CO)_4(\mu\text{-}Cl)_2$, 14523-22-9; $Rh_2Sn_2(CO)_2Cl_6[\mu\text{-}(Ph_2P)_2py]_2$, 98653-03-0; $Rh_2Sn_2(CO)_2Cl_6[\mu\text{-}(Ph_2P)_2py]_2\cdot 2CH_2Cl_2$, 98719-05-2; $SnCl_2$, 7772-99-8; $(Ph_2P)_2py$, 64741-27-1.

Supplementary Material Available: Tables of structure factors, atomic thermal parameters, and hydrogen coordinates for $Rh_2Sn_2(Co)_2Cl_6[\mu\text{-}(Ph_2P)_2py]_2\cdot 1.5CH_2Cl_2$ (26 pages). Ordering information is given on any current masthead page.

(28) The method obtains an empirical absorption tensor from an expression relating F_o and F_c. Hope, H.; Moezzi, B., local program XABS.
(29) "International Tables for X-ray Crystallography"; Kynock Press: Birmingham, England, 1974; Vol. IV.

Mechanistic Polyoxoanion Chemistry: Intramolecular Rearrangements of the α-$Mo_8O_{26}^{4-}$, $C_6H_5AsMo_7O_{25}^{4-}$, and $(C_6H_5As)_2Mo_6O_{24}^{4-}$ Anions[1]

W. G. Klemperer,* C. Schwartz, and D. A. Wright

Contribution from the School of Chemical Sciences, University of Illinois, Urbana, Illinois 61801. *Received April 1, 1985*

Abstract: The dynamic behavior of the α-$Mo_8O_{26}^{4-}$, $C_6H_5AsMo_7O_{25}^{4-}$, and $(C_6H_5As)_2Mo_6O_{24}^{4-}$ anions as $(n\text{-}C_4H_9)_4N^+$ salts in CH_3CN has been studied by using variable-temperature ^{17}O NMR line-shape analysis, ^{17}O spin saturation transfer techniques, and ^{17}O label crossover experiments. The $C_6H_5AsMo_7O_{25}^{4-}$ anion shows two distinct types of fluxional behavior that can be related to the anion's structure, a puckered Mo_6O_{18} ring capped on opposite sides by tridentate tetrahedral MoO_4^{2-} and $C_6H_5AsO_3^{2-}$ units. The low-temperature process involves Mo_6O_{18} ring inversion accompanied by twisting of the $C_6H_5AsO_3^{2-}$ subunit and twisting or flipping of the MoO_4^{2-} subunit. Only weak (>2.2 Å) molybdenum–oxygen bonds are broken and reformed. The higher temperature process, although mechanistically undefined, involves cleavage of stronger (1.7–2.0 Å) molybdenum–oxygen bonds. Evidence is presented for related processes in the α-$Mo_8O_{26}^{4-}$ and $(C_6H_5As)_2Mo_6O_{24}^{4-}$ anions. Possibilities for observing related ring inversions and reorientations of tetrahedral subunits in other early transition-metal polyoxoanions are also discussed.

Almost nothing is known about the detailed reaction mechanisms of early transition-metal polyoxoanion transformations.[2] Despite extensive speculation on the subject, little experimental information is available due to the problem of applying standard mechanistic probes to systems of such great structural complexity. This problem is compounded by the difficulty of synthesizing specific compounds designed to test mechanistic hypotheses. The research reported here partially remedies this situation through the application of ^{17}O dynamic NMR line-shape analysis, ^{17}O spin saturation transfer techniques, and ^{17}O label crossover experiments to mechanistic polyoxoanion chemistry.

The title anions were selected for study on the basis of their common $[(RXO_3^{2-})_2(Mo_6O_{18})]$ structure, **1**, in which RXO_3^{2-} units are tetrahedral $C_6H_5AsO_3^{2-}$ and/or $OMoO_3^{2-}$ anions connected by weak molybdenum–oxygen bonds to opposite sides of an $Mo_6^{VI}O_{18}$ ring. The two key features of structure **1**, its

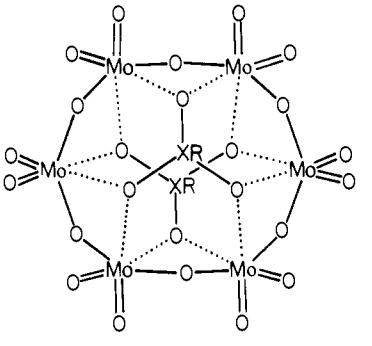

1

tetrahedral oxoanion and neutral Mo_nO_{3n} ring subunits, are of central importance since they are features observed in numerous other early transition-metal polyoxoanion structures. The tetrahedral PO_4^{3-} ion, for example, is a subunit of the Keggin anion

(1) ^{17}O Nuclear Magnetic Resonance Spectroscopy of Polyoxometalates. 3.
(2) Pope, M. T. "Heteropoly and Isopoly Oxometalates"; Springer-Verlag: New York, 1983; pp 136–140.

0002-7863/85/1507-6941$01.50/0

$PMo_{12}O_{40}^{3-}$,[3] the Dawson anion $P_2Mo_{18}O_{62}^{6-}$,[4] and numerous related species. Neutral Mo_nO_{3n} rings are also found in many different structures such as the $P_2Mo_5O_{23}^{6-}$ [5] and $(CH_3)_2AsMo_4O_{15}H^{2-}$ [6] structures (see below). An understanding of dynamic behavior in the case of the title anions therefore has direct relevance to the understanding of dynamic behavior in numerous other systems.

Experimental Section

A. ^{17}O NMR Spectral Measurements. ^{17}O NMR spectra were measured at 33.9 MHz from 12 mm o.d. vertical sample tubes without sample spinning on an unlocked FTNMR system equipped with a 5.87-T Oxford Instruments magnet and a Nicolet NIC-80 data processor. The magnet was shimmed by tuning the probe to ^{133}Cs and observing an aqueous CsI sample. All spectra were externally referenced to 22 °C fresh tap water by the sample replacement method. Chemical shifts are reported as positive numbers for resonances that are observed at high frequency (low field) relative to the reference frequency. A spectral bandwidth of 50 000 Hz was digitized by using 8192 data points. The pulse repetition rate was 2.7 Hz for the spin saturation transfer experiments but 5.88 Hz otherwise. The pulse width used for all spectra measured, 28 μs, corresponded to a 70° pulse.

The spin saturation transfer pulse sequence was a selective 206-ms 3–5-W saturation pulse followed immediately by a nonselective observe pulse, a 20-μs preacquisition delay, and a 164-ms acquisition time. The total recycle time was 370 ms. Due to the high power level of the saturation pulse, off-resonance saturation sometimes occurred when an ^{17}O resonance at frequency ν_A was in the neighborhood of the ^{17}O resonance at frequency ν_B being selectively saturated. The fact that this saturation arose from the high power level, not spin transfer between oxygen sites, was established by irradiating the sample at $2\nu_A - \nu_B$, i.e., at a frequency separated from ν_A by $|\nu_A - \nu_B|$ but not at ν_B. If the degree of saturation of the resonance at ν_A was the same when the sample was irradiated at ν_B and at $2\nu_A - \nu_B$, spin saturation transfer between the oxygen sites was ruled out. The high power level of the saturation pulse also raised the probe temperature by ca. 2 °C. Data were collected only after the probe temperature had equilibrated. The sample temperature was monitored during data acquisition by using a thermocouple built into the probe. This thermocouple was calibrated before and after each set of experiments by placing another thermocouple into a 12-mm sample tube containing acetonitrile, lowering this assembly into the probe, and then equilibrating the system by using a standard variable-temperature apparatus while the spin saturation pulse sequence was applied.

All ^{17}O NMR spectra referred to in the text, table, and figures were measured from 0.03 M acetonitrile solutions of 16 atom % ^{17}O-enriched materials. In all spectra shown in the figures, 7-Hz exponential line broadening was employed. Line widths reported in the table, however, have been corrected for this line broadening. For the $(C_6H_5As)_2Mo_6O_{24}[(n\text{-}C_4H_9)_4N]_4$ sample, 19 000 FID's were accumulated, for $C_6H_5AsMo_7O_{25}[(n\text{-}C_4H_9)_4N]_4$, 10 000, and for $\alpha\text{-}Mo_8O_{26}[(n\text{-}C_4H_9)_4N]_4$, 5000 in saturation transfer experiments, otherwise 3500.

B. Sample Preparation. Reagents, Solvents, and General Procedures. The following were purchased from commercial sources and used without further purification: $Na_2MoO_4{\cdot}2H_2O$ (Fisher); $(n\text{-}C_4H_9)_4NBr$ (Aldrich); concentrated HCl (Mallinckrodt), and ^{17}O-enriched water (Monsanto Research). Phenylarsonic acid (Aldrich) was recrystallized by cooling a room-temperature saturated ethanol–water solution (1:1 by volume) to ca. 0 °C. Unless noted otherwise, CH_3CN was dried by distillation from P_4O_{10} under nitrogen and then stored over activated 3-Å molecular sieves. CD_3CN (MSD isotopes) was stirred over CaH_2 for 24 h and then vacuum-distilled. Diethyl ether (CCI) and toluene (Fisher) were distilled from sodium benzophenone ketyl and stored over activated 4-Å molecular sieves. Molecular sieves (Linde) were activated by heating at 350 °C for at least 24 h and then cooling under vacuum. All dried solvents were stored in a nitrogen-filled drybox until used. All transfers involving anhydrous and ^{17}O-enriched compounds were performed in a nitrogen atmosphere in order to prevent hydration and isotopic dilution, respectively.

Analytical Procedures. Elemental analyses were performed by the University of Illinois School of Chemical Sciences microanalytical laboratory and Galbraith Laboratories, Knoxville, TN. Infrared spectra were measured from mineral oil (Nujol) mulls between KBr plates on a Perkin-Elmer Model 1330 infrared spectrophotometer and were referenced to the 1028-cm^{-1} band of a 0.05-mm polystyrene film. ^1H NMR spectra were recorded at 360 MHz on a Nicolet NT-360 FTNMR spectrometer equipped with a deuterium lock. Chemical shifts were internally referenced to $(CH_3)_4Si$.

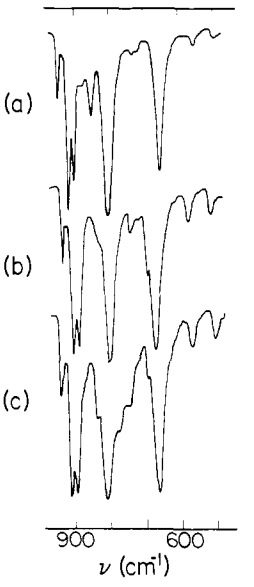

Figure 1. IR spectra of (a) $(\alpha\text{-}Mo_8O_{26})[(n\text{-}C_4H_9)_4N]_4$, (b) $[(C_6H_5As)_2Mo_6O_{24}][(n\text{-}C_4H_9)_4N]_4$, and (c) $(C_6H_5AsMo_7O_{25})[(n\text{-}C_4H_9)_4N]_4$ measured from Nujol mulls between KBr plates. See Experimental Section for numerical data.

$[(C_6H_5As)_2Mo_6O_{24}][(n\text{-}C_4H_9)_4N]_4$. The preparation of this compound is derived from a synthetic procedure developed by Filowitz[7] and a dehydration procedure reported by Pope.[8]

Concentrated aqueous HCl (3.87 mL, 46.4 mmol) was added at a rate of ca. 1 drop/30 s to a rapidly stirring solution of $C_6H_5AsO_3H_2$ (6.35 g, 31.4 mmol) and $Na_2MoO_4{\cdot}2H_2O$ (22.8 g, 94.2 mmol) in 42 mL of deionized water. Stirring was continued for 15 min after the acidification was complete, and a solution of $(n\text{-}C_4H_9)_4NBr$ (20.4 g, 63.3 mmol) in 42 mL of deionized water was then added. The resulting white precipitate was collected by suction filtration, washed thoroughly twice with 100-mL portions of deionized water, washed twice with 75-mL portions of ether, air-dried on a glass first for ca. 1 h, and then stored over P_4O_{10} under vacuum for 1 h. The resulting crude, hydrated product (14 g) was added to 70 mL of boiling CH_3CN (dried over 3-Å molecular sieves), insoluble material was removed by gravity filtration, and the solution volume was reduced to ca. 25 mL by boiling off solvent. Upon cooling to room temperature, plate-shaped crystals of the hydrated salt $[(C_6H_5As)_2Mo_6O_{24}(OH_2)][(n\text{-}C_4H_9)_4N]_4$[8] formed. These crystals (9.4 g) were collected by filtration and stored under vacuum over P_4O_{10} for 24 h. Dehydration was accomplished as follows. The crystalline hydrate was added to 40 mL of CH_3CN in a vial containing a magnetic stirring bar. The vial was then sealed and immersed into an 85 °C oil bath. The resulting clear solution was stirred for 24 h and then cooled to room temperature. The slightly cloudy solution was gravity-filtered and added to ca. 150 mL of ether to yield a white precipitate that was collected by suction filtration and washed twice with 15-mL portions of ether. This precipitate was dissolved into 35 mL of boiling CH_3CN, the resulting solution was gravity-filtered, and ca. 10 mL of CH_3CN was boiled off. Plate-shaped crystals formed upon cooling the solution to room temperature, and the crystals were collected by suction filtration after 15 h at −20 °C and dried in vacuo (6.8 g, 3.0 mmol, 19% yield based on Mo). The analytical sample was crystallized a total of 3 times. Anal. Calcd for $As_2Mo_6O_{24}C_{76}H_{154}N_4$: As, 6.71; Mo, 25.77; C, 40.87; H, 6.95; N, 2.51. Found: As, 6.70; Mo, 25.63; C, 40.85; H, 7.11; N, 2.51. IR (Nujol, 975–475 cm^{-1}, see Figure 1b) 941 (m), 911 (s), 893 (s), 835 (sh, m), 804 (s), 794 (w), 694 (m), 671 (s), 577 (w), 512 (w); ^1H NMR (360 MHz, 22 °C, CD_3CN) δ 8.06–8.09 (m, 4 H), 7.49–7.58 (m, 6 H), cation resonances are at δ 3.10–3.15, 1.57–1.66, 1.31–141, 0.94–0.98.

^{17}O-enriched material was prepared by dissolving 1.0 g of crystalline $[(C_6H_5As)_2Mo_6O_{24}][(n\text{-}C_4H_9)_4N]_4$ into 10 mL of CH_3CN and 220 μL of ^{17}O-enriched water. The solution was stirred at ambient temperature for 1 h and then at 65 °C for 14 h. After cooling to ambient temperature,

(3) Reference 2, p 23.
(4) Reference 2, p 70.
(5) Reference 2, p 28.
(6) Reference 2, p 119.
(7) Filowitz, M. S. Ph.D. Dissertation, Columbia University, New York, 1977.
(8) Kwak, W.; Rajkovic, L. M.; Pope, M. T.; Quicksall, C. O.; Matsumoto, K. Y.; Sasaki, Y. *J. Am. Chem. Soc.* **1977**, *99*, 6463.

solid material was precipitated from solution with ca. 100 mL of ether and collected by suction filtration. This solid was dehydrated and recrystallized by using the procedures outlined above to give 0.410 g of enriched $(C_6H_5As)_2Mo_6O_{24}[(n\text{-}C_4H_9)_4N]_4$ (41% yield).

$(C_6H_5AsMo_7O_{25})[(n\text{-}C_4H_9)_4N]_4$. A 20-mL vial containing a magnetic stirring bar was charged with 0.485 g (0.217 mmol) of $[(C_6H_5As)_2Mo_6O_{24}][(n\text{-}C_4H_9)_4N]_4$, 0.468 g (0.217 mmol) of $(\alpha\text{-}Mo_8O_{26})[(n\text{-}C_4H_9)_4N]_4$,[9] and 6.2 mL of CH_3CN. The vial was sealed, immersed into a 55 °C oil bath, stirred for 11 h, and cooled to room temperature. Ether (40 mL) was slowly added to this clear solution with stirring, yielding an oily semisolid that was solidified by swirling the solution and dispersing the oil by scratching the bottom of the flask with a spatula. The resulting white powder was collected by suction filtration and washed twice with 20-mL portions of ether, yielding 0.774 g of crude product. This crude product was dissolved into 1.8 mL of CH_3CN, and toluene (ca. 7 mL) was added with swirling just until the solution became slightly cloudy. Storing the solution at −20 °C for 24 h yielded plate-shaped crystals that were collected by suction filtration and dried in vacuo (0.420 g, 0.191 mmol, 44% yield).

The analytical sample was crystallized a total of 3 times. Anal. Calcd for $AsMo_7O_{25}C_{70}H_{149}N_4$: As, 3.42; Mo, 30.62; C, 38.33; H, 6.85; N, 2.55. Found: As, 3.33; Mo, 30.51; C, 38.18; H, 6.85; N, 2.55. IR (Nujol 975–475 cm^{-1}, see Figure 1c) 945 (m), 914 (s), 899 (s), 841 (m), 812 (s), 775 (m), 744 (m), 694 (m), 664 (s), 571 (w), 504 (w); ^1H NMR (360 MHz, 22 °C, CD_3CN) δ 8.01–8.05 (m, 2 H), 7.58–7.62 (m, 3 H), cation resonances are at δ 3.12–3.17, 1.57–1.64, 1.34–1.41, and 0.95–0.99.

^{17}O-enriched $[(C_6H_5As)Mo_7O_{25}][(n\text{-}C_4H_9)_4N]_4$ was prepared by the above procedure by using ^{17}O-enriched $\alpha\text{-}Mo_8O_{26}[(n\text{-}C_4H_9)_4N]_4$.[9]

$(\alpha\text{-}Mo_8O_{26})[(n\text{-}C_4H_9)_4N]_4$. The preparation of this material and a procedure for enriching it in ^{17}O are described in ref 9: IR (Nujol, 975–475 cm^{-1}, see Figure 1a) 950 (m), 920 (s), 903 (s), 852 (m), 806 (s), 738 (w), 720 (w), 659 (s), 560 (w), 497 (w).

Results

Line-shape analysis of temperature-dependent NMR spectra is often a simple and versatile method for studying rapid chemical transformations, particularly in diamagnetic systems involving only spin $-\,^1/_2$ nuclei.[10] In this case, chemical exchange is usually the only physical process that significantly affects NMR line shapes as a function of temperature, simplifying spectral analysis. In the case of quadrupolar nuclei like ^{17}O, however, quadrupolar relaxation also affects NMR line widths as a function of temperature,[9] and the effects of chemical exchange and quadrupolar relaxation can consequently be difficult to distinguish experimentally. In certain systems, this difficulty can be circumvented through control of the site-exchange rate by means other than temperature variation.[11] Alternatively, chemical-exchange processes can be probed without varying exchange rates by using spin saturation transfer[12,13] or two-dimensional NMR[14] techniques.

This section is concerned with establishing the solution structures and studying the solution dynamic behavior of the title anions by using ^{17}O dynamic NMR spectroscopy and ^{17}O label crossover experiments. The specific objective is the delineation of oxygen site exchange schemes characterizing this behavior. Mechanistic questions will be addressed in the Discussion section.

Solution Structures. The solid-state structures of $\alpha\text{-}Mo_8O_{26}^{4-}$ and $(CH_3As)_2Mo_6O_{24}^{4-}$ have been determined X-ray crystallographically.[15,16] Both D_{3d} anions contain tridentate oxoanions, MoO_4^{2-} or $CH_3AsO_3^{2-}$, bonded to opposite sides of a puckered Mo_6O_{18} ring by weak (2.3–2.6 Å) molybdenum–oxygen bonds (see **1**). Within the Mo_6O_{18} rings, bond distances from molybdenum to terminal OMo oxygens and doubly-bridging OMo_2 oxygens are

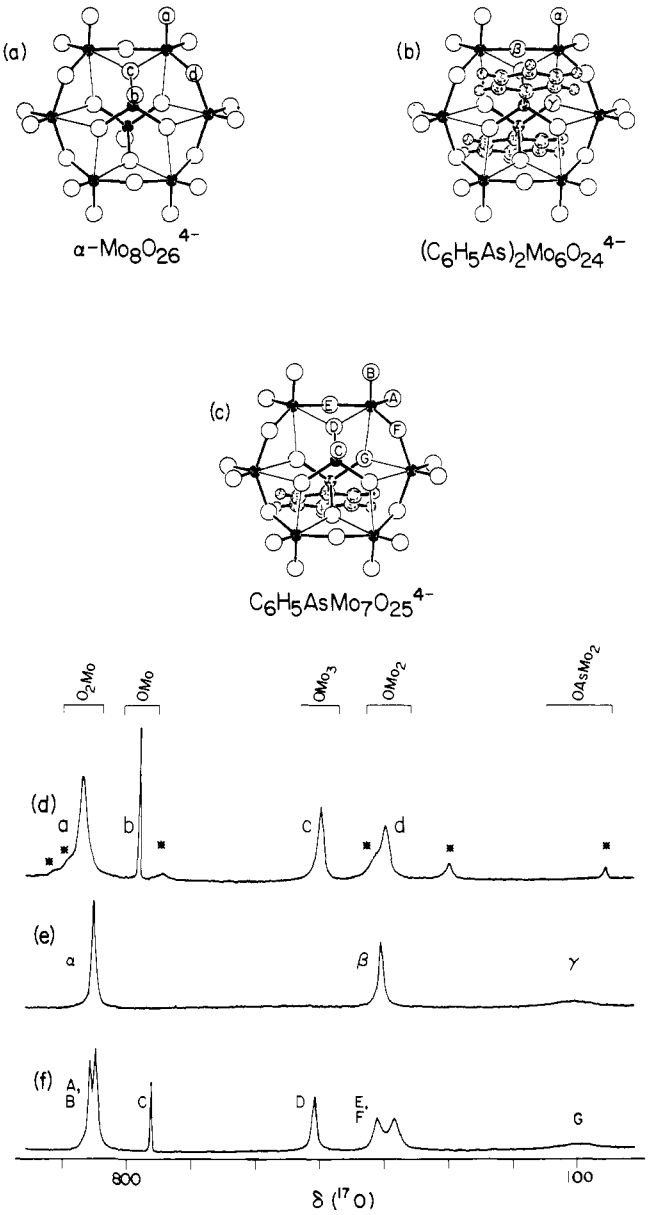

Figure 2. SCHAKAL drawings of (a) $\alpha\text{-}Mo_8O_{26}^{4-}$, (b) $(C_6H_5As)_2Mo_6O_{24}^{4-}$, and (c) $C_6H_5AsMo_7O_{25}^{4-}$. Atoms in the C_6H_5As groups are represented by shaded circles, oxygen atoms by open circles, and molybdenum atoms by filled circles. One member from each set of nonequivalent oxygen atoms is labeled. Oxygen-17 NMR spectra of these anions are shown in (d)–(f). See the text for an explanation of the assignment schemes, Table I for numerical data, and the Experimental Section for experimental conditions.

1.66–1.72 and 1.88–1.93 Å, respectively. In light of these considerations the $\alpha\text{-}Mo_8O_{26}^{4-}$ and $(CH_3As)_2Mo_6O_{24}^{4-}$ anions can be formulated structurally as $[(MoO_4^{2-})_2(Mo_6O_{18})]$ and $[(CH_3AsO_3^{2-})_2(Mo_6O_{18})]$, respectively.

When $\alpha\text{-}Mo_8O_{26}[(n\text{-}C_4H_9)_4N]_4$ is dissolved in CH_3CN, an equilibrium is established between $\alpha\text{-}Mo_8O_{26}^{4-}$ and $\beta\text{-}Mo_8O_{26}^{4-}$.[17] The ^{17}O NMR spectrum of $\alpha\text{-}Mo_8O_{26}^{4-}$ in CH_3CN shown in Figure 2d therefore contains resonances, marked with asterisks, arising from $\beta\text{-}Mo_8O_{26}^{4-}$.[9,15b] Resonances arising from the O_2Mo and OMo_2 oxygens in $\alpha\text{-}Mo_8O_{26}$ (O_a and O_d in Figure 2a, respectively) are assigned as indicated in Figure 2d by comparison of their chemical shift values with those for resonances assigned to corresponding oxygens in $(C_6H_5As)_2Mo_6O_{24}^{4-}$ (see below). The two remaining resonances in the $\alpha\text{-}Mo_8O_{26}^{4-}$ spectrum, labeled b and c in Figure 2d, are assigned to the OMo and OMo_3 oxygens, respectively, on the basis of their relative intensities. Note that

(9) Filowitz, M.; Ho, R. K. C.; Klemperer, W. G.; Shum, W. *Inorg. Chem.* **1979**, *18*, 93.
(10) Sandstrom, J. "Dynamic NMR Spectroscopy"; Academic Press: London, 1982; p 6–29.
(11) Jackson, J. A.; Taube, H. *J. Phys. Chem.* **1965**, *69*, 1844.
(12) Reference 10, pp 53–64.
(13) Martin, M. L.; Martin, G. J.; Delpuech, J.-J. "Practical NMR Spectroscopy"; Heyden: London, 1980; pp 315–321.
(14) Jeener, J.; Meier, B. H.; Bachmann, P.; Ernst, R. R. *J. Chem. Phys.* **1979**, *71*, 4546.
(15) (a) Fuchs, J.; Hartl, H. *Angew. Chem., Int. Ed. Engl.* **1976**, *15*, 375. (b) Day, V. W.; Fredrich, M. F.; Klemperer, W. G.; Shum, W. *J. Am. Chem. Soc.* **1977**, *99*, 952.
(16) Kwak, W.; Rajkovic, L. M.; Stalick, J. K.; Pope, M. T.; Quicksall, C. O. *Inorg. Chem.* **1976**, *15*, 2778.
(17) Klemperer, W. G.; Shum, W. *J. Am. Chem. Soc.* **1976**, *98*, 8291.

Table I. ^{17}O NMR (33.9 MHz) Spectral Data for $(C_6H_5As)_2Mo_6O_{24}^{4-}$, α-$Mo_8O_{26}^{4-}$, and $C_6H_5AsMo_7O_{25}^{4-}$ [a]

anion and temp, °C	chemical shifts[b] (line widths[c])				
	O_2Mo	OMo	OMo_3	OMo_2	$OAsMo_2$
$(C_6H_5As)_2$-$Mo_6O_{24}^{4-}$	842			398	103
−15	(455)			(542)	([d])
+5	(304)			(385)	(3170)
+22	(237)			(296)	(2472)
+83	(147)			(192)	(1411)
α-$Mo_8O_{26}^{4-}$	865	777	497	397	
−15	(437)	(43)	(346)	(663[e])	
+4	(270)	(275)	(335)	(372)	
+22	(228)	(836)	(557)	(367)	
+45	(319)	([d])	(2496)	(795[e])	
$C_6H_5AsMo_7O_{25}^{4-}$	853, 844	760	507	410, 380	101
+1	(609[f])	(12)	(321)	(409), (480)	([d])
+20	(529[f])	(42)	(240)	(1378[f])	(2370)
+33	(504[f])	(140)	(254)	(1044[g])	(2158)
+62	(479[f])	([d])	(857)	(435[g])	(1407)
+70	(489[f])	([d])	(926)	(449[g])	(1162)
+88	(508[f])	([d])	([d])	(714[g])	(1119)

[a] See Experimental Section for spectral parameters and experimental conditions. [b] See text and figures for assignments. Chemical shifts, given in ppm, are temperature-independent within experimental error. Errors associated with chemical shift values are ±2 ppm for $\nu_{1/2} < 300$ Hz, ±3 ppm for 300 Hz $< \nu_{1/2} <$ 700 Hz, and ±8 ppm for $\nu_{1/2} > 700$ Hz. [c] Linewidths fwhm, given in hertz, are enclosed in parentheses. Errors associated with line-width values are ±15 Hz for $\nu_{1/2} < 200$ Hz, ±30 Hz for 200 Hz $< \nu_{1/2} <$ 550 Hz, ±80 Hz for 550 Hz $< \nu_{1/2} <$ 1100 Hz, and ±15% for $\nu_{1/2} > 1100$ Hz. [d] Resonance too broad to measure with meaningful accuracy. [e] Line width is accurate only to ±150 Hz due to overlap with β-$Mo_8O_{26}^{4-}$ resonance. [f] Combined line width of two resonances at half-height of more intense resonance. [g] Line width of coalesced resonance.

the overall assignment scheme yields the expected[9] pattern of larger downfield chemical shifts for oxygens with shorter O–Mo bonds.

The $(C_6H_5As)_2Mo_6O_{24}^{4-}$ anion is isostructural with the $(CH_3As)_2Mo_6O_{24}^{4-}$ anion described above, according to IR spectroscopic data,[8] and therefore contains only three nonequivalent oxygens, labeled α–γ in Figure 2b. Its ^{17}O NMR spectrum, assigned as indicated in Figure 2e,[18] is completely consistent with the proposed structure.

The $C_6H_5AsMo_7O_{25}^{4-}$ anion, reported here for the first time, is prepared as an $[(n\text{-}C_4H_9)_4N]^+$ salt according to reaction 1 and formulated from its elemental composition and ^1H NMR spectrum (see Experimental Section). Reaction 1 can be monitored by

$$(C_6H_5As)_2Mo_6O_{24}^{4-} + \alpha\text{-}Mo_8O_{26}^{4-} \rightarrow 2C_6H_5AsMo_7O_{25}^{4-} \quad (1)$$

^1H NMR spectroscopy and requires about 24 h to reach completion (<3% reactant) at ambient temperature in dry acetonitrile. As shown in Figure 1, the IR spectrum of this new anion bears a close resemblance to IR spectra of the α-$Mo_8O_{26}^{4-}$ [17,19] and $(C_6H_5As)_2Mo_6O_{24}^{4-}$ [8] anions, suggesting the structure shown in Figure 2c and the structural formulation $[(C_6H_5AsO_3^{2-})(MoO_4^{2-})(Mo_6O_{18})]$. The ^{17}O NMR spectrum shown in Figure 2f is completely consistent with this structure. Resonances for all nonequivalent oxygens are resolved and have chemical shift values similar to values for resonances assigned to oxygens in α-$Mo_8O_{26}^{4-}$ and $(C_6H_5As)_2Mo_6O_{24}^{4-}$ having similar structural environments.

Solution Dynamics: $(C_6H_5As)_2Mo_6O_{24}^{4-}$. Variable-temperature ^{17}O NMR spectra of $[(C_6H_5As)_2Mo_6O_{24}][(n\text{-}C_4H_9)_4N]_4$ in CH_3CN illustrate the dependence of ^{17}O NMR line widths upon temperature expected in the absence of chemical exchange and spin–spin coupling effects (see Table I). In this case, line widths are controlled by quadrupolar relaxation according to eq 2,[21] where

$$\nu_{1/2} = \frac{1}{\pi T_2} = \frac{1}{\pi T_1} = \frac{3}{125\pi}\left(1 + \frac{\eta^3}{3}\right)\left(\frac{e^2Qq}{\hbar}\right)\tau_c \quad (2)$$

η is the electric field gradient asymmetry parameter, $(e^2Qq/\hbar)$ is the quadrupolar coupling constant, and τ_c is the correlation time for molecular rotation. All the terms in eq 2 are independent of temperature except τ_c. Assuming rapid isotropic molecular rotation in a homogeneous medium, an assumption implicit in eq 2, τ_c is independent of the nuclear site within a given rigid molecule or ion and decreases with increasing temperature. As a result, ^{17}O NMR line widths decrease with increasing temperature, and the same fractional decrease in line width is observed for all resonances arising from nuclei within a given rigid species. Consider, for example, the decrease in ^{17}O NMR line widths for $(C_6H_5As)_2Mo_6O_{24}^{4-}$ upon raising the sample temperature from +5 to +22 °C: within experimental error, the line width of each resonance at +22 °C is 78% of its value at +5 °C.

Since variable-temperature ^{17}O NMR spectra of the $(C_6H_5As)_2Mo_6O_{24}^{4-}$ anion show no chemical-exchange broadening between −15 and +83 °C, rapid oxygen site exchange between O_2Mo, OMo_2, and $OAsMo_2$ oxygens can be ruled out. Note, however, that this behavior is consistent with any rapid exchange process that exchanges oxygens between symmetry-equivalent oxygen sites.

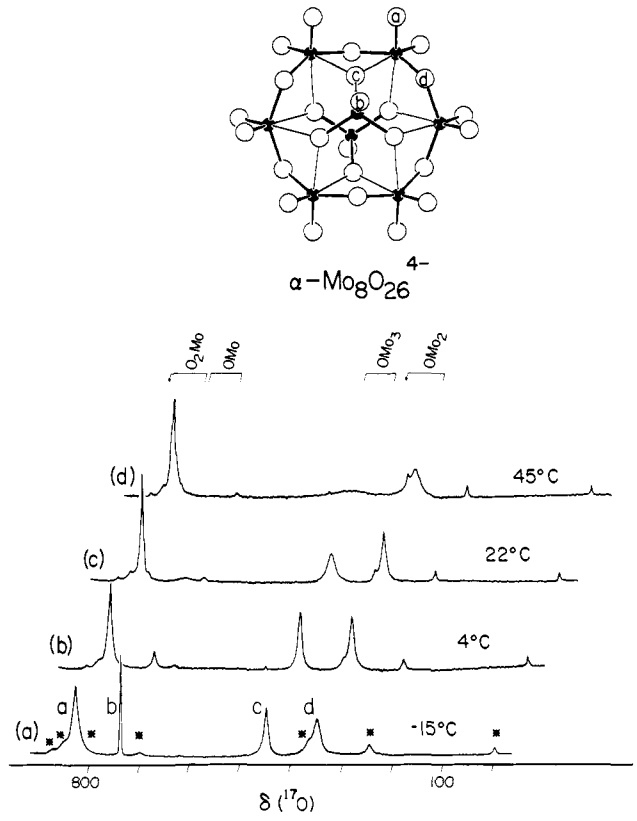

Figure 3. Variable-temperature 33.9-MHz ^{17}O NMR spectra of $(\alpha$-$Mo_8O_{26})[(n\text{-}C_4H_9)_4N]_4$ in CH_3CN. For details, see text and Table I. The SCHAKAL drawing of α-$Mo_8O_{26}^{4-}$ is labeled as indicated in the Figure 2 caption.

Solution Dynamics: α-$Mo_8O_{26}^{4-}$. Oxygen-17 NMR spectra of α-$Mo_8O_{26}[(n\text{-}C_4H_9)_4N]_4$ measured at four different temperatures in CH_3CN are shown in Figure 3. Relevant chemical shift and line-width data are summarized in Table I. Three different types of temperature-dependent line-width variations are apparent: (1) the O_2Mo and OMo_2 resonances narrow with increasing

(18) Filowitz, M.; Klemperer, W. G. *J. Chem. Soc., Chem. Commun.* **1976**, 233.

(19) The IR spectra of α-$Mo_8O_{26}[(n\text{-}C_4H_9)_4N]_4$ reported here and in ref 17 differ significantly from the spectrum reported in ref 20. The spectrum reported in ref 20 can be reproduced by allowing pure, solid $(\alpha$-$Mo_8O_{26})[(n\text{-}C_4H_9)_4N]_4$ to react with water vapor before measuring its IR spectrum.

(20) Fuchs, J.; Brüdgam, I. *Z. Naturforsch., B* **1977**, *32B*, 853.

(21) Abragam, A. "Principles of Nuclear Magnetic Magnetism"; Oxford University Press: London, 1961; p 314.

temperature from −15 to +4 °C but begin to broaden with increasing temperature somewhere between +4 and +45 °C; (2) the OMo_3 resonance maintains approximately constant line width between −15 and +4 °C but becomes increasingly broad as the temperature is raised above 4 °C; (3) the OMo resonance becomes broader with increasing temperature over the entire temperature range studied. This type of temperature dependence clearly cannot be explained by quadrupole relaxation alone, and chemical-exchange phenomena must be invoked.

Before considering chemical-exchange processes involving only α-$Mo_8O_{26}^{4-}$ that can account for the behavior just described, two physically plausible processes involving other species in solution must be ruled out. First, rapid interconversion of α-$Mo_8O_{26}^{4-}$ and β-$Mo_8O_{26}^{4-}$ can be ruled out since ^{17}O NMR resonances from β-$Mo_8O_{26}^{4-}$ in equilibrium with α-$Mo_8O_{26}^{4-}$ all narrow as the sample temperature is raised from −15 to +45 °C (see Figure 3).[22] Second, water exchange[25] can be ruled out since ^{17}O–^1H spin–spin coupling is retained in ^{17}O resonances from water added to the α-$Mo_8O_{26}^{4-}$ solutions under discussion. Even at 54 °C, the water resonance can be observed as a triplet.

The problem of identifying chemical-exchange broadening in the presence of quadrupolar broadening is apparent from comparison of the α-$Mo_8O_{26}^{4-}$ ^{17}O NMR line widths at −15 and +4 °C (see Table I). The OMo resonance is exchange-broadened at +4 °C by at least 232 = 275 − 43 Hz, and OMo oxygens are thus undergoing rapid exchange with some other type(s) of α-$Mo_8O_{26}^{4-}$ oxygens. It is impossible, however, to determine which type of oxygens are exchanging with the OMo oxygens. Less-rapid quadrupole relaxation causes all α-$Mo_8O_{26}^{4-}$ resonances besides the OMo resonance to narrow with increasing temperature between −15 and +4 °C, overriding at least in part the line broadening which might be caused by chemical exchange. This dilemma can be resolved by performing spin saturation transfer experiments.

Transfer of spin saturation to a given nuclear site can be observed only if the rate of transfer is at least about as rapid as the rate of quadrupolar relaxation at that site. The effectiveness of spin saturation transfer from site B to site A in a two-site system is given by eq 3,[12,13] where $I_A°$ is the intensity of resonance A when

$$\frac{I_A}{I_A°} = \frac{R_A}{k_A + R_A} \tag{3}$$

resonance B has not been saturated, I_A is the intensity of resonance A after resonance B has been saturated for a time period sufficiently long to achieve magnetization equilibrium in the system, R_A is the rate of quadrupole relaxation $(1/T_1)$ for nuclei at site A, and k_A is the first-order rate constant for spin transfer from site A to site B. Clearly, saturation transfer to a given site can be observed only if the rate of spin transfer from that site (k_A) approaches or exceeds that of quadrupolar relaxation at that site (R_A). Practically speaking, spin saturation transfer to the most severely quadrupole-broadened resonances is the most difficult to detect experimentally.

The effect of selectively irradiating each of the nonequivalent α-$Mo_8O_{26}^{4-}$ oxygens to saturation at 4 °C is shown in Figure 4.

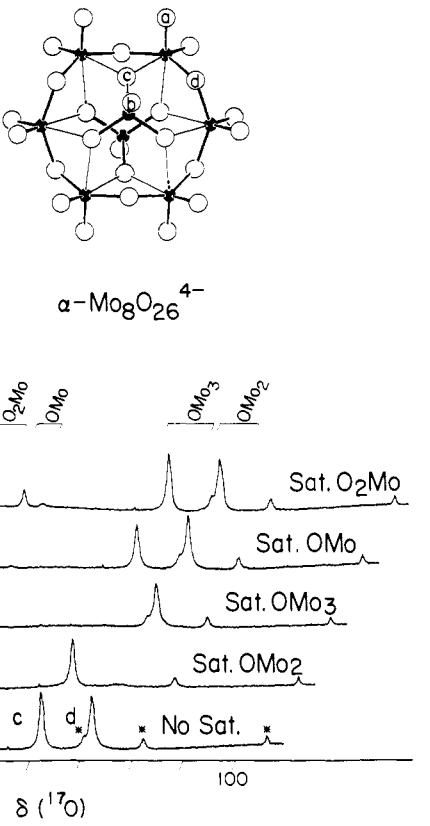

Figure 4. ^{17}O NMR spectrum (33.9-MHz) of $(\alpha\text{-}Mo_8O_{26})[(n\text{-}C_4H_9)_4N]_4$ in CH_3CN at 4 °C is shown in (a). Spectra (b)–(e) were obtained under the same conditions immediately following selective saturation of the resonance indicated (see Experimental Section). The SCHAKAL drawing of α-$Mo_8O_{26}^{4-}$ is labeled as indicated in the Figure 2 caption.

These spectra show spin saturation transfer in only two instances: saturation of the OMo_3 oxygen nuclei is effectively transferred to the OMo oxygen site, causing the OMo oxygen resonance to disappear (Figure 3c); saturation of the OMo oxygen nuclei is partially transferred to the OMo_3 oxygen site, causing the OMo_3 oxygen resonance to suffer a ca. 20% loss of intensity. The site-exchange scheme responsible for exchange broadening of α-$Mo_8O_{26}^{4-}$ resonances at 4 °C therefore involves only two sites, the OMo and OMo_3 oxygen sites.

At temperatures above 4 °C, the OMo and OMo_3 resonances show the expected dynamic NMR behavior; i.e., both broaden with increasing temperature, with the OMo resonance broadening more rapidly than the OMo_3 resonance. The O_2Mo and OMo_2 resonances, on the other hand, show qualitative temperature-dependent line-width behavior between −15 and +22 °C attributable to quadrupolar relaxation. At some temperature between 4 and 45 °C, however, both of these resonances broaden with increasing temperature, indicating the onset of a second chemical-exchange process involving O_2Mo and OMo_2 oxygens.

Solution Dynamics: $C_6H_5AsMo_7O_{25}^{4-}$. Variable-temperature ^{17}O NMR spectra of $C_6H_5AsMo_7O_{25}[(n\text{-}C_4H_9)_4N]_4$ in CH_3CN are shown in Figure 5. Comparison of the line widths observed for $C_6H_5AsMo_7O_{25}^{4-}$ resonances at different temperatures reveals several different trends (see Table I): (1) the $OAsMo_2$ resonance consistently narrows with increasing temperature; (2) the OMo resonance consistently broadens with increasing temperature until it is too broad to detect; (3) the OMo_3 resonance narrows with increasing temperature between 1 and ca. 20 °C, has an approximately constant line width between 20 and ca. 35 °C, and at higher temperatures broadens with increasing temperature; (4) the two OMo_2 resonances broaden as the temperature is raised above 0 °C until they coalesce to a single resonance at 31.5 ± 1.5 °C, and this resonance narrows with increasing temperature until 62 ± 2 °C, at which point it broadens with increasing temperature; (5) the two O_2Mo resonances both narrow with in-

(22) Rapid interconversion of α-$Mo_8O_{26}^{4-}$ and β-$Mo_8O_{26}^{4-}$ in CH_3CN was proposed by Masters et al.[23] on the basis of ^{95}Mo NMR spectra of $(\alpha\text{-}Mo_8O_{26})[(n\text{-}C_4H_9)_4N]_4$ in CH_3CN and $(\beta\text{-}Mo_8O_{26})(K)[(n\text{-}C_4H_9)_4N]_3$ in CH_3CN. Both spectra showed a single resonance 15 ppm downfield from MoO_4^{2-}. Since (1) both solutions are known to contain α-$Mo_8O_{26}^{4-}$ as a major or minor component,[17] (2) α-$Mo_8O_{26}^{4-}$ contains tetrahedral Mo^{VI} centers but β-$Mo_8O_{26}^{4-}$ does not, and (3) tetrahedral Mo^{VI} centers yield sharp ^{95}Mo resonances but distorted octahedral Mo^{VI} centers do not,[24] Masters et al. probably observed ^{95}Mo resonances for tetrahedral Mo^{VI} centers in α-$Mo_8O_{26}^{4-}$ in both solutions but failed to detect the resonances for octahedral Mo^{VI} centers in both α- and β-$Mo_8O_{26}^{4-}$ due to their large line widths. See: Gheller, S. F.; Sidney, M.; Masters, A. F.; Brownlee, R. T. C.; O'Connor, M. J.; Wedd, A. G. *Aust. J. Chem.* **1984**, *37*, 1825.

(23) Masters, A. F.; Gheller, S. F.; Brownlee, R. T. C.; O'Connor, M. J.; Wedd, A. G. *Inorg. Chem.* **1980**, *19*, 3866.

(24) Kautt, W. D.; Krüger, H.; Lutz, O.; Maier, H.; Nolle, A. *Z. Naturforsch., A* **1976**, *31a*, 351.

(25) In aqueous solution, oxygen exchange between water and $Mo_8O_{26}^{4-}$ is rapid on the NMR time scale (see ref 9).

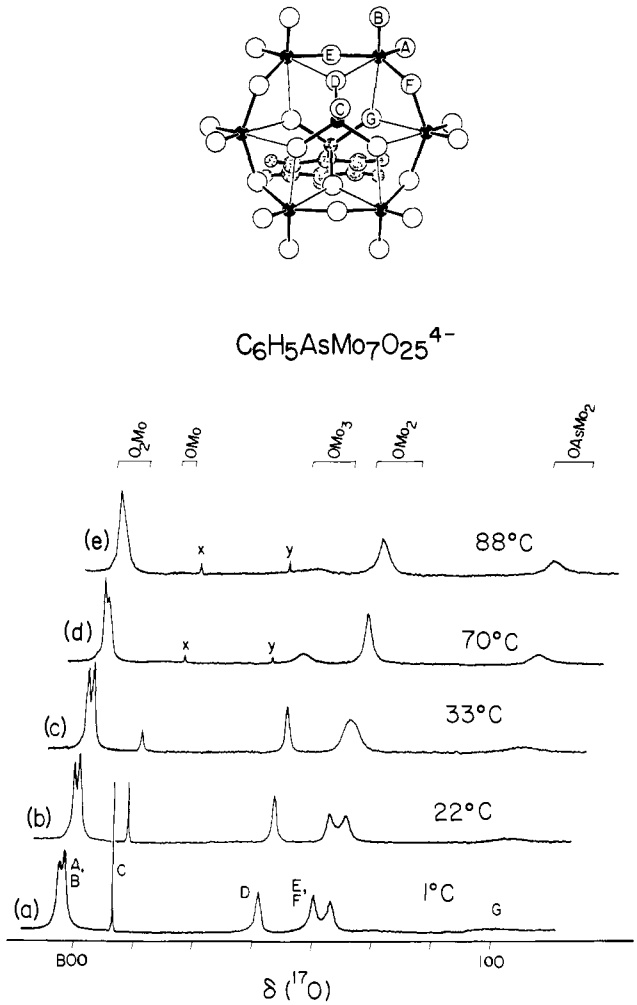

Figure 5. Variable-temperature 33.9-MHz ^{17}O NMR spectra of $(C_6H_5AsMo_7O_{25})[(n\text{-}C_4H_9)_4N]_4$ in CH_3CN. For details, see text and Table I. The SCHAKAL drawing of $C_6H_5AsMo_7O_{25}^{4-}$ is labeled as indicated in the Figure 2 caption.

creasing temperature between 0 and 58 ± 2 °C and broaden at higher temperatures, but the upfield resonance clearly broadens to a greater degree than the downfield resonance. At temperatures above ca. 60 °C, two new resonances appear, labeled x and y in Figure 5d and e. Resonance x appears at 716 ppm and is assigned to the terminal oxygen in $Mo_2O_7^{2-}$.[9] Resonance y appears at 564 ppm and is assigned to the bridging oxygens in $Mo_6O_{19}^{2-}$.[9] Both resonances disappear upon cooling to 22 °C. These species might arise from $C_6H_5AsMo_7O_{25}^{4-}$ thermal decomposition, traces of water attacking $C_6H_5AsMo_7O_{25}^{4-}$, or α-$Mo_8O_{26}^{4-}$ impurities.[26] Water, however, is not involved in any rapid-exchange processes. When 3 equiv of water is added to 0.03 M $C_6H_5AsMo_7O_{25}[(n\text{-}C_4H_9)_4N]_4$ in CH_3CN, a narrow water triplet is observed in ^{17}O NMR spectra at temperatures as high as 76 °C.

In the 0–33 °C temperature range, four nonequivalent types of oxygens are involved in site exchanges sufficiently rapid to affect NMR line widths: the OMo and OMo_3 oxygens bonded to the tetrahedral molybdenum centers and the two types of OMo_2 oxygens bridging between octahedral molybdenum centers. The nature of the site exchange processes responsible for this line broadening is clarified by the results of spin saturation transfer experiments performed at 33 °C. No spin saturation transfer is observed upon saturation of the O_2Mo, OMo, OMo_2, or $OAsMo_2$ nuclei, but saturation of the OMo_3 nuclei results in complete saturation of the OMo nuclei, i.e., disappearance of the OMo resonance. This establishes an exchange process between the OMo and OMo_3 oxygens analogous to the one observed in α-$Mo_8O_{26}^{4-}$. A separate process is responsible for the broadening of the two OMo_2 resonances, mutual exchange between the two OMo_2 oxygen sites, since the coalesced OMo_2 resonance narrows as the temperature increases from 33 to 75 °C, a feature inconsistent with rapid exchange between OMo_2 and OMo or OMo_3 oxygens.

The relative rates of the two site exchange processes just described can be estimated by independently calculating first-order rate constants for OMo/OMo_3 oxygen exchange and OMo_2 mutual exchange at the coalescence temperature for the two OMo_2 oxygen resonances, T_c = 31.5 ± 1.5 °C. Given that the line width of the OMo resonance at 0 °C is only 12 Hz, the line width at T_c, 120 ± 20 Hz,[27] arises almost exclusively from exchange broadening. Upper and lower limits for exchange broadening can therefore be set at 140 = 120 + 20 and 88 = 120 − 20 − 12 Hz. This in turn places upper and lower limits for k_{OMo} at 440 = 140π s^{-1} and 276 = 88π s^{-1}, i.e., k_{OMo} = 358 ± 82 s^{-1} at T_c. A value of the first-order rate constant for OMo_2 mutual exchange, k_{OMo_2} = 1.85 ± 0.15 × 10^3 s^{-1}, is obtained from line-shape simulations.[28] The rate constant k_{OMo_2} is therefore 4–7 times larger than the rate constant k_{OMo}.

Like the α-$Mo_8O_{26}^{4-}$ ion, the $C_6H_5AsMo_7O_{25}^{4-}$ ion displays additional dynamic behavior involving exchange between O_2Mo and OMo_2 oxygen sites at elevated temperatures. Unlike the OMo_2 oxygens at lower temperatures, however, the O_2Mo oxygens do not undergo mutual exchange; i.e., the two O_2Mo resonances do not broaden and coalesce as the sample temperature is raised above 33 °C. Instead, they broaden independently, with the upfield resonance broadening more rapidly than the downfield resonance.

Crossover Experiments. Both the α-$Mo_8O_{26}^{4-}$ and $C_6H_5AsMo_7O_{25}^{4-}$ anions contain tetrahedral MoO_4^{2-} moieties that are linked to octahedral molybdenum centers by six very long bonds (see above), and dynamic NMR experiments just described indicate that nonequivalent OMo and OMo_3 oxygens within the MoO_4^{2-} subunits are undergoing rapid mutual site exchange at ambient temperature. If one assumes that very long bonds are also very labile bonds, the observed site exchange can be accounted for by rapid reorientation of rigid MoO_4^{2-} units as a whole relative to the remainder of the α-$Mo_8O_{26}^{4-}$ or $C_6H_5AsMo_7O_{24}^{4-}$ structure. This could occur either intramolecularly or intermolecularly according to eq 4 and 5. If eq 4 and 5 are operative, exchange of

$$[(MoO_4^{2-})_2(Mo_6O_{18})] = [(MoO_4^{2-})(Mo_6O_{18})] + MoO_4^{2-} \quad (4)$$

$$[(C_6H_5AsO_3^{2-})(MoO_4^{2-})(Mo_6O_{18})] = [(C_6H_5AsO_3^{2-})(Mo_6O_{18})] + MoO_4^{2-} \quad (5)$$

MoO_4^{2-} subunits between α-$Mo_8O_{26}^{4-}$ and $C_6H_5AsMo_7O_{25}^{4-}$ should be easily detected by an ^{17}O-labeling experiment in which oxygens in ^{17}O-enriched α-$Mo_8O_{26}^{4-}$ are exchanged with oxygens in unenriched $C_6H_5AsMo_7O_{25}^{4-}$.

Dry acetonitrile solutions of ^{17}O-enriched $(\alpha\text{-}Mo_8O_{26})[(n\text{-}C_4H_9)_4N]_4$ and unenriched $(C_6H_5AsMo_7O_{25})[(n\text{-}C_4H_9)_4N]_4$, prepared in a 1:2 mole ratio for ease of ^{17}O observation, require well over 30 min at 60 °C to exchange completely to a statistical ^{17}O distribution, thus ruling out eq 4 and 5 as the mechanisms for rapid MoO_4^{2-} reorientation. One can in this fashion rigorously rule out an intermolecular mechanism for MoO_4^{2-} reorientation in both anions but cannot rigorously rule out the possibility of an intermolecular mechanism for one anion and an intramolecular mechanism for the other anion.[30] In light of the close structural

(26) The α-$Mo_8O_{26}^{4-}$ and $C_6H_5AsMo_7O_{25}^{4-}$ ions can cocrystallize as $(n\text{-}C_4H_9)_4N^+$ salts and are therefore difficult to separate. The α-$Mo_8O_{26}^{4-}$ resonance appearing as an 864-ppm shoulder in ^{17}O NMR spectra of $C_6H_5AsMo_7O_{25}[(n\text{-}C_4H_9)_4N]_4$ in CH_3CN at elevated temperatures could arise from sample contamination, hydrolysis, decomposition, and/or equilibration of $C_6H_5AsMo_7O_{25}^{4-}$ with α-$Mo_8O_{26}^{4-}$ and $(C_6H_5As)_2Mo_6O_{24}^{4-}$. Rapid oxygen exchange between α-$Mo_8O_{26}^{4-}$ and $C_6H_5AsMo_7O_{25}^{4-}$ is ruled out, however, by ^{17}O label crossover experiments described below.

(27) The uncertainty here arises from uncertainty in T_c.

(28) The Gutowsky-Holm equation[29] was used (NMCXCH on a Nicolet 1280 computer), allowing $(\pi T_2)^{-1}$ to vary between 225 and 400 Hz. The uncertainty in k_{OMo} arises from uncertainty in T_2.

(29) Rogers, M. T.; Woodbrey, J. C. *J. Phys. Chem.* **1962**, *66*, 540.

Scheme I

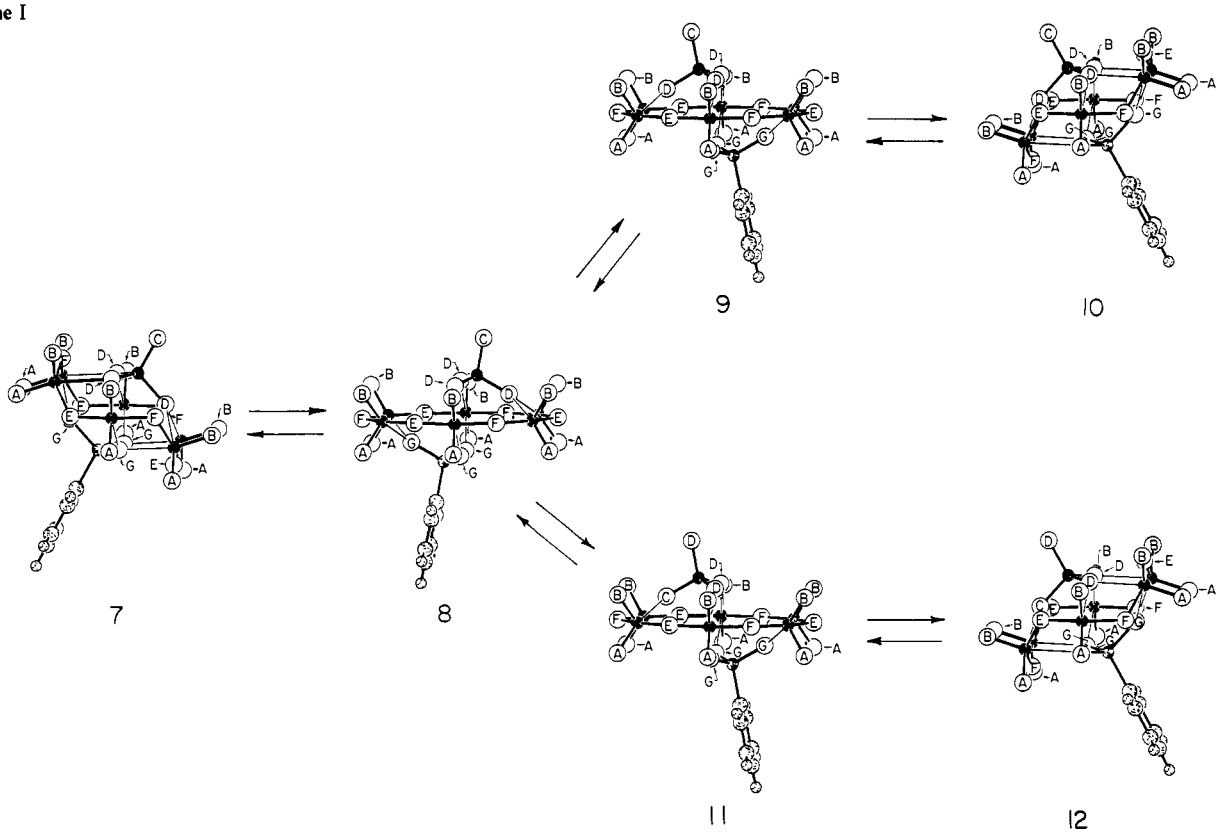

analogies between the two anions noted above and the similar rates for MoO_4^{2-} reorientation in the two systems, we regard the failure to observe rapid MoO_4^{2-} transfer as establishing an intramolecular mechanism for MoO_4^{2-} reorientation in both α-$Mo_8O_{26}^{4-}$ and $C_6H_5AsMo_7O_{25}^{4-}$.

Since the ^{17}O-labeling experiments just described were performed at 60 °C, the conclusions drawn are relevant not only to the mechanism of OMo_3/OMo exchange but also to the mechanisms of higher temperature exchange processes discussed above. All processes which are measurably rapid on the NMR time scale at 60 °C are intramolecular, and the α-$Mo_8O_{26}^{4-}$ and $C_6H_5AsMo_7O_{25}^{4-}$ anions are truly fluxional species.

Discussion

In the preceding section, the results of dynamic NMR experiments were used to define site exchange schemes describing rapid intramolecular rearrangements of the α-$Mo_8O_{26}^{4-}$ and $C_6H_5AsMo_7O_{25}^{4-}$ anions. In this section, these site exchange schemes will be translated into mechanisms, and an attempt will be made to extend these mechanisms to related systems that have the potential for displaying similar dynamic behavior. Discussion will deal exclusively with the low-temperature processes observed for $C_6H_5AsMo_7O_{25}^{4-}$ and α-$Mo_8O_{26}^{4-}$ involving site exchange between oxygens bonded to tetrahedrally coordinated molybdenum centers and, in the case of $C_6H_5AsMo_7O_{25}^{4-}$, mutually exchange between OMo_2 oxygens linking octahedrally coordinated Mo centers. The high temperature exchange processes involving O_2Mo and OMo_2 oxygens will not be discussed since these site exchanges are not sufficiently well-defined to allow mechanistic interpretation.

$C_6H_5AsMo_7O_{25}^{4-}$. Two distinct intramolecular site exchanges are detectable by dynamic NMR experiments, a rapid mutual exchange between nonequivalent OMo_2 oxygens and a slightly slower exchange between OMo and OMo_3 oxyens. These are easily seen to correspond to simple structural reorganizations by dissecting the $C_6H_5AsMo_7O_{25}^{4-}$ structure into $C_6H_5AsO_3^{2-}$, MoO_4^{2-}, and Mo_6O_{18} subunits as discussed above (see **1**) and assuming that the weakest bonds in the structure, those interconnecting the subunits, are also the most labile bonds. Then the OMo_2 exchange process corresponds to Mo_6O_{18} ring inversion, and the OMo/OMo_3 exchange corresponds to MoO_4^{2-} reorientation. Discussion here will begin with the mechanism of the more rapid ring inversion process and then turn to the mechanism of tetrahedral reorientation.

An appealingly simple pathway for Mo_6O_{18} ring inversion proceeds via a configuration where the six molybdenum centers and six OMo_2 bridging oxygens are approximately coplanar. There is precedent for such ring configuration in the $[(CH_3AsO_3^{2-})(Mo_6O_{18})(H_2O)_6]$ structure,[32] **2**. A second structure, the

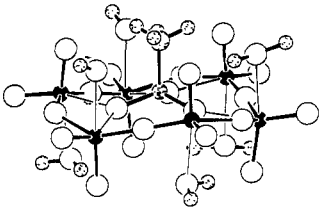

2

$[(C_6H_5AsO_3^{2-})_2(Mo_6O_{18})(H_2O)]$ structure[33] shown in **3**,[34] suggests a mechanism for achieving a planar Mo_6O_{18} ring configuration in $C_6H_5AsMo_7O_{25}^{4-}$. Comparison of structure **3** with the $[(CH_3AsO_3^{2-})_2(Mo_6O_{18})]$ structure,[16] **4**,[34] shows it to be derived from **4** by cleavage of two very weak (2.3–2.5 Å) molybdenum–

(30) Ideally, the rates of eq 5 and 6 could be probed individually by performing ^{18}O crossover experiments between an ^{18}O-enriched sample and an unenriched sample of the same anion and detecting ^{18}O crossover by mass spectroscopy, specifically, by fast atom bombardment mass spectroscopy (FABMS). Such experiments are not feasible using current FABMS methodology since the proven low-volatility matrices decompose $(\alpha\text{-}Mo_8O_{26})[(n\text{-}C_4H_9)_4N]_4$ and $(C_6H_5AsMo_7O_{25})[(n\text{-}C_4H_9)_4N]_4$. Unfortunately, only a restricted class of early transition-metal polyoxoanions can be examined by FABMS due to the fairly drastic sampling conditions involved.[31]

(31) Finke, R. G.; Droege, M. W.; Cook, J. C.; Suslick, K. S. *J. Am. Chem. Soc.* **1984**, *106*, 5750.
(32) Matsumoto, K. Y. *Bull. Chem. Soc. Jpn.* **1979**, *52*, 3284.
(33) Matsumoto, K. Y. *Bull. Chem. Soc. Jpn.* **1978**, *51*, 492.
(34) Phenyl and methyl groups are represented by large, shaded spheres in **3** and **4** for purposes of clarity.

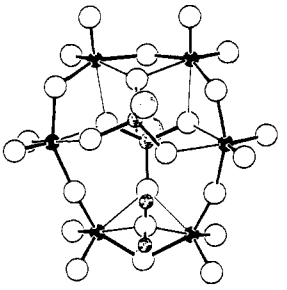

3

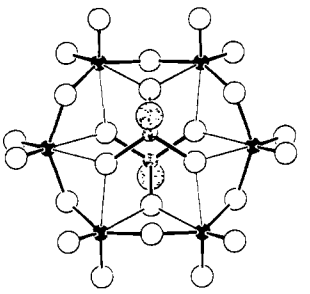

4

oxygen bonds in **4** and formation of two new, very weak [2.393 (14) and 2.478 (15) Å[33]] molybdenum–oxygen bonds to the water molecule in **3**. This change in connectivity is of course accompanied by a conformational change in the Mo_6O_{18} ring subunit, a change that is seen clearly when the $[(C_6H_5AsO_3^{2-})_2(Mo_6O_{18})(H_2O)]$ structure is viewed from the perspective shown in **5**. Here, four of the molybdenums together with five of the

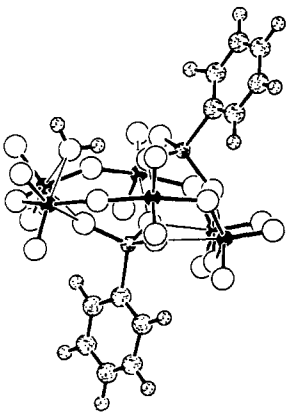

5

OMo_2 bridging oxygens in the Mo_6O_{18} ring subunit are seen to be almost coplanar.[35] All of the Mo_6O_{18} molybdenums and bridging oxygens can be placed in an approximately planar configuration by adding a second water molecule to the opposite side of the Mo_6O_{18} ring of **4** in a symmetric fashion to yield the hypothetical, approximately C_{2h} $[(C_6H_5AsO_3^{2-})_2(Mo_6O_{18})(H_2O)_2]$ anion, **6**. If the weakly-bound water molecules in **6** are removed

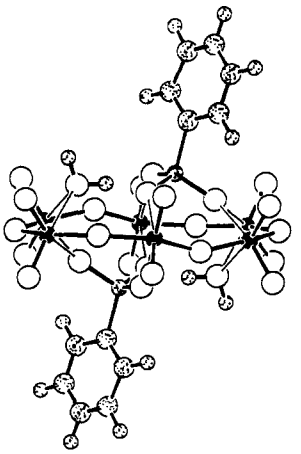

6

and one $C_6H_5AsO_3^{2-}$ subunit is replaced by an MoO_4^{2-} subunit, an attractive idealized intermediate configuration for ring inversion in $C_6H_5AsMo_7O_{25}^{4-}$ is obtained (see **8** in Scheme I).

(35) The deviations from planarity can be traced to a hydrogen-bonding interaction between one of the coordinated water's protons and one of the OAsMo oxygens (see structure **3**).

In Scheme I, the reactant $C_6H_5AsMo_7O_{25}^{4-}$ configuration **7** shown on the far left is labeled by using the same scheme employed in Figures 2c and 5. These labels are retained as the reactant configuration is transformed to the product configurations 10 and 12 through the intermediate configurations **8**, **9**, and **11**. Note that **7**, **10**, and **12** are indistinguishable if the labels are ignored, as are **8**, **9**, and **11**. Returning to the proposed mechanism of ring inversion in $C_6H_5AsMo_7O_{25}^{4-}$, it must effect mutual exchange of the O_E and O_F oxygens in **7**. Although the idealized Mo_6O_{18} ring subunit in **8** is planar and has C_{2h} symmetry, the overall configuration including MoO_4^{2-} and $C_6H_5AsO_3^{2-}$ subunits has only C_s symmetry and thus nonequivalent O_F and O_E oxygens. If both the $C_6H_5AsO_3^{2-}$ and MoO_4^{2-} subunits are reoriented relative to the Mo_6O_{18} ring, however, the O_E and O_F oxygens can be made equivalent. We shall first consider reorientation of the $C_6H_5AsO_3^{2-}$ subunit. The $C_6H_5AsO_3^{2-}$ unit can move from its position in **8** to its position in **9** and **11** by rotating 30° about its pseudothreefold rotation axis as it translates from one end of the Mo_6O_{18} ring to the other. It is interesting to note that the beginnings of precisely such a rotation/translation, i.e., twist, are evident in the structure of the $[(C_6H_5AsO_3^{2-})_2(Mo_6O_{18})(H_2O)]$ anion (see **3**). Here, the structure is distorted from C_s symmetry by a hydrogen-bonding interaction between the coordinated water molecule and one of the $C_6H_5AsO_3^{2-}$ oxygens. The MoO_4^{2-} subunit can of course reorient with the same twisting motion, and the **8** to **9** transformation accomplishes O_E–O_F site exchange via $C_6H_5AsO_3^{2-}$ and MoO_4^{2-} twists. After **9** is transformed to **10** by the reverse of the **7** to **8** transformation, the overall **7** to **8** to **9** to **10** transformation is seen to effect O_E/O_F exchange and only O_E/O_F exchange. Unlike the $C_6H_5AsO_3^{2-}$ unit that can reorient itself only by a twist mechanism, the MoO_4^{2-} can reorient itself by a flip mechanism as shown in the **8** to **11** transformation. Although the MoO_4^{2-} flip involves more rotation than the twist and is therefore not the least motion pathway, it does involve fewer bond-breaking and bond-making steps. In contrast to the twist mechanism, it leads to O_C/O_D exchange, and the overall site exchange process for the **7** to **12** transformation is therefore O_E/O_F exchange plus O_C/O_D exchange. Recalling from above that the rate of mutual exchange between OMo oxygens (O_E/O_F exchange) is about 5 times faster than the rate of exchange between OMo and OMo_3 sites (O_C/O_D exchange), the MoO_4^{2-} twist mechanism (**8** to **9**) is actually favored over the MoO_4^{2-} flip mechanism (**8** to **11**) by a factor of about 5 in terms of rates.

Since the plausibility of Scheme I as a mechanism for intramolecular rearrangement in $C_6H_5AsMo_7O_{25}^{4-}$ rests upon the plausibility of the intermediate configurations shown in **8**, **9**, and **11**, two precedents for key features of this structure should be mentioned. First, polyoxomolybdate rings containing square-pyramidal five-coordinate Mo^{VI} centers adjacent to octahedral six-coordinate centers are known and have been characterized X-ray crystallographically in two carbomolydates, the $HCCHMo_4O_{15}F^{3-}$ and $HCCHMo_4O_{17}CH^{3-}$ anions.[36] Second, the oval-shaped, planar $Mo_6^{VI}O_6$ ring in **8** and the corresponding $Nb_6^{V}O_6$ ring in the $Nb_8O_{10}(OCH_2C_6H_5)_{20}$ structure[37] **13** have strikingly similar dimensions. Moreover, the gross similarities between the hexagonally close-packed oxygen arrangement in **13** and the only slightly less regular oxygen arrangement in **8** cannot escape the eye.

α-$Mo_8O_{26}^{4-}$ and $(C_6H_5As)_2Mo_6O_{24}^{4-}$. Since the α-$Mo_8O_{26}^{4-}$ and $(C_6H_5As)_2Mo_6O_{24}^{4-}$ anions are closely related to the $C_6H_5AsMo_7O_{25}^{4-}$ anion by simply interchanging MoO_4^{2-} and $C_6H_5AsO_3^{2-}$ subunits, it is natural to inquire whether they undergo rapid intramolecular rearrangement in a related manner, i.e., according to Scheme I. In the case of α-$Mo_8O_{26}^{4-}$, rapid site exchange is observed between OMo and OMo_3 oxygens bonded to the tetrahedral molybdenum centers, and following the same line of reasoning just given for the $C_6H_5AsMo_7O_{25}^{4-}$ case, a

(36) Day, V. W.; Thompson, M. R.; Day, C. S.; Klemperer, W. G.; Liu, R.-S. *J. Am. Chem. Soc.* **1980**, *102*, 5971.

(37) (a) Riley Schaefer, private communiction. (b) Cf. $Nb_8O_{10}(OC_2H_5)_{20}$: Bradley, D. C.; Hursthouse, M. B.; Rodesiler, P. F. *J. Chem. Soc., Chem. Commun.* **1968**, 1112.

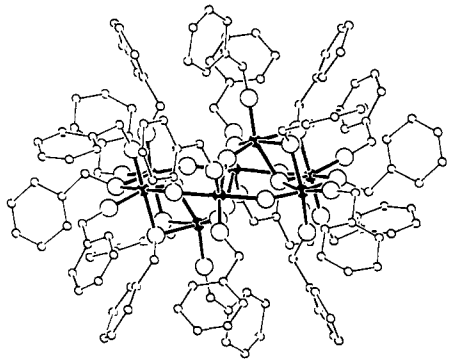

13

mechanism of the type shown in Scheme I can be invoked. Unfortunately, however, ring inversion cannot be observed experimentally by ^{17}O NMR, because all OMo_2 bridging oxygens in α-$Mo_8O_{26}^{4-}$ are symmetry-equivalent, and ring inversion thus implies no oxygen site exchange. In the case of $(C_6H_5As)_2Mo_6O_{24}^{4-}$, neither Mo_6O_{18} ring inversion nor $C_6H_5AsO_3^{2-}$ twisting of the type shown in Scheme I imply an oxygen site exchange observable by ^{17}O NMR, and there is therefore no evidence whatsoever for fluxional behavior in $(C_6H_5As)_2Mo_6O_{24}^{4-}$.

To address the question of whether α-$Mo_8O_{26}^{4-}$ and $C_6H_5AsMo_7O_{25}^{4-}$ undergo rapid intramolecular rearrangements of the type shown in Scheme I, one must therefore resort to indirect, as opposed to direct, evidence. Specifically, one must return to the transformation of $[(C_6H_5AsO_3^{2-})_2(Mo_6O_{18})]$ (**4**) to its water adduct, $[(C_6H_5AsO_3^{2-})_2(Mo_6O_{18})(H_2O)]$ (**3**). Since the Mo–O bonds formed in **3** upon addition of water have about the same length as the bonds broken in **4** upon addition of water, the driving force for this transformation is in all probability not the formation of stronger metal–oxygen bonds. Instead, it probably reflects the greater stability of the Mo_6O_{18} ring subunit in a planar conformation than in a puckered conformation. It is likely therefore that transformations of the type **7** to **8** occur easily in α-$Mo_8O_{26}^{4-}$ and $(C_6H_5As)_2Mo_6O_{24}^{4-}$. Furthermore, since the $C_6H_5AsO_3^{2-}$ subunit is easily twisted in **3** as a response to a hydrogen-bonding interaction with the bound water molecule as discussed above, $C_6H_5AsO_3^{2-}$ and MoO_4^{2-} twists of the type shown in the **8** to **9** and **8** to **11** transformations probably are facile in general. In summary, available evidence gives every reason to believe that both α-$Mo_8O_{26}^{4-}$ and $(C_6H_5As)_2Mo_6O_{24}^{4-}$ easily undergo rapid ring inversion and MoO_4^{2-} and/or $C_6H_5AsO_3^{2-}$ reorientation of the type shown in Scheme I.

Generalizations: Tetrahedral Subunit Reorientations. Having observed intramolecular reorientations of tetrahedral MoO_4^{2-} subunits in α-$Mo_8O_{26}^{4-}$ and $C_6H_5AsMo_7O_{25}^{4-}$, it is natural to inquire whether other polyoxoanions or even three-dimensional lattice compounds that contain relatively isolated tetrahedral subunits might also undergo facile reorientation. Of the large number of candidates for such behavior,[38,39] we shall discuss only two cases, the α-$PW_{12}O_{40}^{3-}$ [40] and α-A-$PW_9O_{34}^{9-}$ [41] anions, that illustrate the directions in which the present study might be extended.

The α-$PW_{12}O_{40}^{3-}$ or $[(PO_4^{3-})(\alpha\text{-}W_{12}O_{36})]$ anion has the T_d α-Keggin structure in which a tetrahedral PO_4^{3-} unit is connected by 12 weak, 2.4-Å[40] tungsten–oxygen bonds to a surrounding $W_{12}O_{36}$ cage (see **14** and **15** in Scheme II). Within this cage, tungsten centers are located at the vertices of a T_d-distorted cuboctahedron and are each bonded to four doubly bridging oxygens ($d_{W\text{-}O}$ = 1.9 Å[40]) and one terminal oxygen ($d_{W\text{-}O}$ = 1.7 Å[40]). Because this T_d cage does not have the full O_h symmetry of a

Scheme II

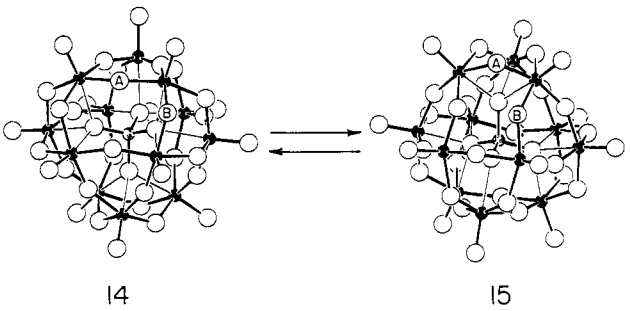

14 15

Scheme III

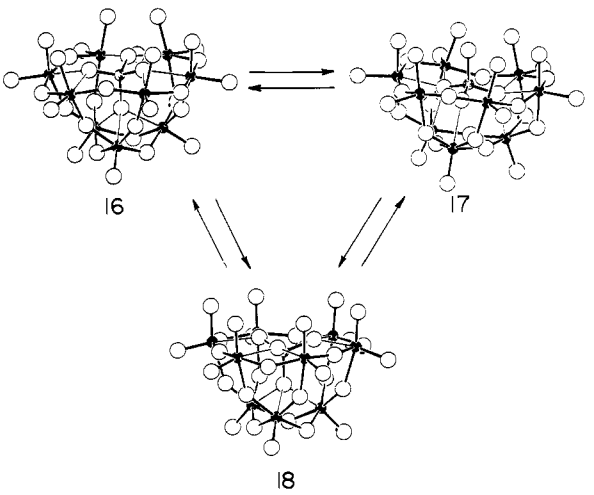

16 17

18

Scheme IV

19 20

cuboctahedron, there are two nonequivalent types of bridging oxygens in α-$PW_{12}O_{40}^{3-}$, labeled A and B in **14** (see Scheme II). By rotating the PO_4^{3-} subunits in α-$PW_{12}O_{40}^{3-}$ 90° about its C_2 axis and allowing the $W_{12}O_{36}$ cage to change its conformation, one achieves the degenerate isomerization shown in Scheme II. This PO_4^{3-} rotation causes the O_A and O_B oxygens to exchange sites. Relative to MoO_4^{2-} reorientation in α-$Mo_8O_{26}^{4-}$ and $C_6H_5AsMo_7O_{25}^{4-}$, PO_4^{3-} reorientation in α-$PW_{12}O_{40}^{3-}$ is a slow process if it occurs at all, since distinct ^{17}O NMR resonances are observed for O_A and O_B oxygens in α-$PW_{12}O_{40}^{3-}$, even at elevated temperatures.[9] This is not surprising since, as Linnett has pointed out,[42] the PO_4^{3-} and $W_{12}O_{36}$ oxygens in α-$PW_{12}O_{40}^{3-}$ form a close-packed array. Note that PO_4^{3-} reorientations of the type shown in Scheme II allow interconversion of isomeric, substituted $PW_{12}O_{40}^{3-}$ ions. The α-1,2-$PV_2W_{10}O_{40}^{5-}$ ion,[43] for example, could isomerize to α-1,4-$PV_2W_{10}O_{40}^{5-}$ in this fashion. This type of isomerization has not been observed to date, a fact that may represent thermodynamic as opposed to kinetic factors since the isomerization is not degenerate.

The isomeric $PW_9O_{34}^{9-}$ ions shown in Scheme III are all derived from $PW_{12}O_{40}^{3-}$ ions by removal of a triangle of three tungsten centers, their three terminal oxygens, and the three doubly bridging oxygens that interconvert them. The α-A-$PW_9O_{34}^{9-}$ (**16**) and α-B-$PW_9O_{34}^{9-}$ (**17**) isomers, for example, are seen to be derived

(38) Reference 2, pp 23–29, 59–81, 118–127.
(39) Wells, A. F., Ed. "Structural Inorganic Chemistry"; Clarendon Press: Oxford, 1975.
(40) Brown, G. M.; Noe-Spirlet, M.-R.; Busing, W. R.; Levy, H. A. *Acta Crystallogr., Sect. B* **1977**, *B33*, 1038.
(41) Reference 2, pp 67–68 and references cited therein.
(42) Linnett, J. W. *J. Chem. Soc.* **1961**, 3796.
(43) Domaille, P. J. *J. Am. Chem. Soc.* **1984**, *106*, 7677.

from the α-$PW_{12}O_{40}^{3-}$ structure by removal of $W_3O_6^{6+}$ units from the top of **14** and **15**, respectively, shown in Scheme II. The β-A-$PW_9O_{34}^{9-}$ isomer, **18**, is derived from the β-$PW_{12}O_{40}^{3-}$ structure in a similar fashion.[44] The three isomers shown in Scheme III can all be interconverted by reorientation of the PO_4^{3-} unit within the $W_9O_{30}^{6-}$ framework. The α-A-$PW_9O_{34}^{9-}$ isomer (**16**) is converted to the α-B-$PW_9O_{34}^{9-}$ isomer (**17**) by rotation of the PO_4^{3-} unit 90° about any one of its local C_2 axes (cf. Scheme II). The α-A-$PW_9O_{34}^{9-}$ isomer (**16**) is converted to the β-A-$PW_9O_{34}^{9-}$ isomer (**18**) by rotation of the PO_4^{3-} unit 60° about the anion's C_3 axis. Note that the PO_4^{3-} units in $PW_9O_{34}^{6-}$ isomers, in contrast to the PO_4^{3-} unit in the α-$PW_{12}O_{40}^{3-}$ anion, are no longer encapsulated within cages and are therefore relatively mobile. The processes shown in Scheme III are likely to be observable under the appropriate experimental conditions, and we believe that they provide a mechanistic basis for the $PW_9O_{34}^{9-}$ transformations described by Finke et al.[45] and Knoth et al.[46]

Generalizations: $(MO_3)_n$ Ring Inversion. The present study has provided detailed evidence for rapid intramolecular Mo_6O_{18} ring inversion in $C_6H_5AsMo_7O_{25}^{4-}$. Numerous other compounds containing larger or smaller $M_n^{VI}O_{3n}$ ring subunits are known that might undergo similar rearrangements.[47] As representative species, we have selected the $(CH_3)_2AsMo_4O_{15}H^{2-}$ [32,48,49] and $(C_6H_5P)_2W_5O_{21}^{4-}$ [50] anions.

The C_{2v} $(CH_3)_2AsMo_4O_{15}H^{2-}$ anion, **19**, contains $(CH_3)_2AsO_2^-$ and OH^- subunits connected by weak bonds to opposite sides of an Mo_4O_{12} ring and can be structurally formulated $\{[(CH_3)_2AsO_2^-](Mo_4O_{12})(OH^-)\}$ see Scheme IV). The Mo_4O_{12} ring subunit is puckered and could undergo ring inversion if the inversion were synchronized with a 90° rotation of the $(CH_3)_2AsO_2^-$ unit about the anion's C_2 axis. This degenerate isomerization exchanges the sites of the OMo_2 bridging oxygens labeled O_A and O_B in Scheme IV. Ring inversion, if it occurs, is relatively slow, however, since the ^{17}O NMR spectrum of $(CH_3)_2AsMo_4O_{15}H^{2-}$ at 80 °C shows two well-resolved resonances for OMo_2 oxygens.[9]

The $(C_6H_5P)_2W_5O_{21}^{4-}$ anion contains two $C_6H_5PO_3^{2-}$ subunits connected by weak bonds to opposite sides of a W_5O_{15} ring and can be structurally formulated $[(C_6H_5PO_3^{2-})_2(W_5O_{15})]$ (see **21**).

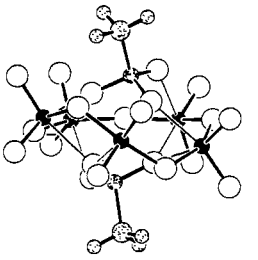

21

As has been pointed elsewhere by others,[50] the W_5O_{15} ring is puckered and could undergo ring inversion if the inversion were accompanied by twisting of the $C_6H_5PO_3^{2-}$ subunits. Although there is no direct evidence for ring inversion in terms of rate-dependent NMR line-shape behavior, the ^{183}W and ^{17}O solution NMR spectra reported for $(C_6H_5P)_2W_5O_{21}^{4-}$ are consistent with fluxional behavior that is immeasurably rapid on the NMR time scale.[50]

Acknowledgment. W.G.K. acknowledges the National Science Foundation for partial support of this research. NMR experiments were performed at the University of Illinois NSF Regional Facility (Grant CHE 79-16100). Preliminary experiments were performed by M. Filowitz, C. Besecker, and M. Diebold. We are grateful to Prof. Riley Schaeffer for providing unpublished $Nb_8O_{10}(OCH_2C_6H_5)_{20}$ coordinates and Prof. Egbert Keller for providing a copy of his SCHAKAL program.

Registry No. $[(C_6H_5As)_2Mo_6O_{24}][(n\text{-}C_4H_9)_4N]_4$, 60187-14-6; $[(C_6H_5As)Mo_7O_{24}][(n\text{-}C_4H_9)_4N]_4$, 98509-06-9; $(\alpha\text{-}Mo_8O_{26})[(n\text{-}C_4H_9)_4N]_4$, 59054-50-1; ^{17}O, 13968-48-4.

(44) Reference 2, p 59.
(45) Finke, R. G.; Droege, M.; Hutchinson, J. R.; Gansow, O. *J. Am. Chem. Soc.* **1981**, *103*, 1587.
(46) Knoth, W. H.; Domaille, P. J.; Farlee, R. D. *Organometallics* **1985**, *4*, 62.
(47) Reference 2, pp 21-23, 43-46, 71-72, 118-123.
(48) Rosenheim, A.; Bileckei, R. *Chem. Ber.* **1913**, *4*, 543.
(49) Barkiga, K. M.; Rajkovic-Blazer, L. M.; Pope, M. T.; Prince, E.; Quicksall, C. O. *Inorg. Chem.* **1980**, *19*, 2531.
(50) Sethuraman, P. R.; Leparulo, M. A.; Pope, M. T.; Zonnevijlle, F.; Brevard, C.; Lemerle, J. *J. Am. Chem. Soc.* **1981**, *103*, 7665.

X-ray Crystal Structure and Conformational Analysis of Tetradecamethylcycloheptasilane, $(Me_2Si)_7$

Fathieh Shafiee, James R. Damewood, Jr., Kenneth J. Haller, and Robert West*

Contribution from the Department of Chemistry, University of Wisconsin, Madison, Wisconsin 53706. *Received May 16, 1985*

Abstract: The crystal and molecular structure of tetradecamethylcycloheptasilane (**1**) has been determined. Crystals of **1** are monoclinic, space group $P2_1/c$ (a = 16.936 Å, b = 10.851 Å, c = 16.451 Å, β = 114.52°). Molecules of **1** are of approximate C_2 symmetry and adopt a twist-chair conformation. Empirical force field (EFF) calculations indicate that while cycloheptane and **1** adopt similar twist-chair ground-state structures, these molecules show significant differences in the structures of other possible conformations (chair, twist-boat, and boat) and the barriers to their interconversion. The average Si-Si-Si angle in **1** (116.2°) is larger than that found for other cyclosilanes.

The family of compounds known as permethylated cyclopolysilanes of general formula $[Si(CH_3)_2]_n$ (where n = 4-35)[1] are of interest for a number of reasons. Of particular interest is the fact that these compounds show unique electronic and spectroscopic properties[2,3] arising from electron delocalization in the σ-framework. For example, they readily form delocalized anion[4] and cation[5] radicals and charge-transfer complexes with π-acceptors.[6]

(1) For reviews see: (a) Gilman, H.; Schwebke, G. L. *Adv. Organomet. Chem.* **1964**, *1*, 89. (b) Kumada, M.; Tamao, K. *Ibid.* **1968**, *6*, 19. (c) West, R.; Carberry, E. *Science* **1975**, *189*, 179. (d) Hengge, E. In "Homoatomic Rings, Chains and Macromolecules of Main-Group Elements"; Rheingold, R. Ed.; Elsevier: Amsterdam, 1977; p 235. (e) West, R. In "Comprehensive Organometallic Chemistry"; Wilkinson, G.; Stone, F. G. A.; Abel, E. W., Eds.; Pergamon Press: Oxford, 1982; Chapter 9.4, p 365.
(2) (a) Pitt, C. G. In "Homoatomic Rings, Chains and Macromolecules of Main-Group Elements"; Rheingold, A., Ed.; Elsevier: Amsterdam, 1977; p 203. (b) West, R. *Pure Appl. Chem.* **1982**, *54*, 1041.
(3) (a) Brough, L. F.; West, R. *J. Am. Chem. Soc.* **1981**, *103*, 3049. (b) Brough, L. F.; West, R. *J. Organomet. Chem.* **1980**, *194*, 139.
(4) Carberry, E.; West, R.; Glass, G. E. *J. Am. Chem. Soc.* **1969**, *91*, 5446.
(5) Bock, H.; Kaim, W.; Kira, M.; West, R. *J. Am. Chem. Soc.* **1979**, *101*, 7667.

0002-7863/85/1507-6950$01.50/0